GEOPHYSICAL TRANSACTIONS 1983
Vol. 29. No. 4. pp. 345-361

TIME DOMAIN IP EQUIPMENT AND METHOD FOR SOURCE DISCRIMINATION

József CSÖRGEI, András ERKEL, László VERŐ*

New results in IP have been presented mostly in the frequency domain with a short comment on the time domain. Data processing and interpretation problems of time domain laboratory and field measurements performed by a broad-band digital tape recorder are discussed here. A brief technical description of the equipment is given, followed by the data processing method based on the Marquardt algorithm. Decay curves measured in a very wide time interval are approximated by the sum of exponential terms. Distributions of amplitudes and time constants for laboratory and field measurements are presented. Measurements performed on rock samples and on geologically controlled sources serve as a basis for interpretation. The method may also permit removal of EM coupling.

d: IP method, time domain, curve shape analysis

1. Introduction

In recent years it has become quite obvious to geophysicists working on the time domain IP that the shape of decay curves could yield information on different physical and material parameters of mineralization or, in other words: different types of sources (sulphide or graphite) produce different decay curves. It is obviously unsatisfactory to compare the curves and declare that "this is similar to that, the other is different". Moreover a qualitative comparison is by no means simple. It is made difficult by the fact that decay curves have no characteristic points, like minima or maxima. Attempts have been made to transform these characterless curves into easily comparable secondary curves by mathematical methods. One of these methods is the differentiation of the decay curves [KOMAROV et al. 1979]. It has been demonstrated by laboratory measurements that the derivatives have a maximum and that the maximum can be found at different moments for different rocks (see *Fig. 1*). The rock samples were chosen in such a way that they could be characterized by only one type of mineralization, e.g. disseminated. Because of this the application of the method under field conditions is not so effective because ore bodies are mainly of mixed type, consequently the derivative of the measured curves ($\tilde{P}$) may have two or more rather uncertain maxima. The measurement itself is cumbersome, the decay curves need to be recorded over a very long period of time and the derivatives, measured or calculated, are very noisy.

There are two different ways for decay curve shape analysis:

i. A theoretical physical—chemical model ought to be found so that the

* Eötvös Loránd Geophysical Institute of Hungary, POB 35, Budapest, H—1440
Paper read at the 43rd Meeting of the European Association of Exploration Geophysicists, Venice, May 1981

very complex induced polarization phenomena can be described completely and so that the values of parameters of the theoretical model can be determined from field data. In this case parameters have a direct physical meaning.

ii. The other possibility is to describe mathematically the shape of decay curves by a certain number of parameters having no physical meaning.

The first of these seems to be more attractive, promising a direct solution for the main task, i.e. source discrimination. Wong's theoretical work do establish a good physical—chemical model for IP [WONG 1979]. It contains, however, a number of parameters. Wong's model and other models using slightly different approaches can be reduced to the Cole—Cole impedance formulation, widely used in the interpretation of complex resistivity data [PELTON et al. 1978]. The computation of the decay curves on the basis of the Cole—Cole model runs into difficulties. The inverse problem, i.e. the determination of the Cole—Cole parameters from time domain IP data is an even more complicated task. Although it is possible to relate the Cole—Cole parameters theoretically to physical properties of rocks, this procedure needs an empirical basis too.

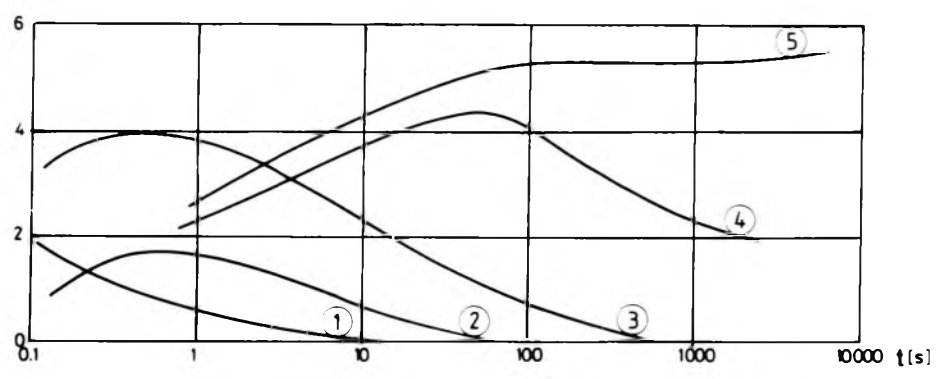

Fig. 1. Time derivatives of decay curves ($\tilde{P}$) measured on rock samples
1 — loose rocks; 2 — barren crystalline rocks; 3 — rocks with fine dissemination of sulphide, graphite and other electrically conductive minerals; 4 — disseminated sulphide ore; 5 — massive ore, veins

1. ábra. Kőzetmintákon mért lecsengési görbék idő szerinti deriváltjai ($\tilde{P}$)
1 — laza kőzet; 2 — kristályos kőzetek, ércmentes; 3 — kőzetek finoman hintett szulfidokkal, grafittal vagy más elektromosan jól vezető ásványokkal; 4 — hintett szulfidos érc; 5 — masszív érc, érctelérek

Рис. 1. Производные замеренных на образцах пород кривых затухания по времени ($\tilde{P}$)
1 — рыхлая порода; 2 — кристаллические породы без руды; 3 — породы с мелко вкрапленными сульфидами, графитом или другими электрически хорошо проводящими минералами; 4 — вкрапленная сульфидная руда; 5 — рудное тело, жилы

Because of the above features, our choice is the second of the two, viz. the pure, as much as possible simple mathematical representation of measured time domain IP data and the experimental determination of the dependence of mathematical parameters on mineralization types.

Mathematically speaking, decay curves are monotonically decreasing functions to be approximated by polynomial or exponential terms, among others. Returning to the well-known formula of WAIT [1959] we suppose that measured apparent polarizability values (P_t) can be described by using the expression

$$P_t = w_0 + \sum_{i=1}^{N} w_i \exp(-t/\tau_i) \tag{1}$$

where w_0 is a constant
w_i, τ_i are the exponential parameters
t is the time after current turn-off
N is the number of exponential terms.

Our aim is to get the so-called dynamic parameters (common name for w_0, w_i and τ_i).

Recently, computer programs based on the Marquardt algorithm have successfully been applied to solve different inversion problems. We have had good results in using the method for obtaining dynamic parameters. The only problem is the need for a relatively large computer memory if many data are used. But we have to use very many data, because we are working in a very wide time interval and more than 10 data/decade are necessary for good approximation. If we have 100—150 data and we are looking for 5—6 exponential terms, that is, 11—13 parameters, a computer of about 60 kbyte memory needs to be used (e.g. HP 9845).

2. The equipment

The equipment used in field and laboratory measurements is a four-channel digital tape recorder. Only certain technical data are mentioned in order to make distinction between the well-known instruments and our equipment.

— The sampling time series is quasi-logarithmic

$$t_{kj} = 2^k(1 + 0.1j)t_{00} \tag{2}$$

where t_{kj} is the sampling time of serial number kj
k is an integer, can be set between 0 and 13, to determine the length of the current-on and current-off intervals
j is an integer between 0 and 9
t_{00} is the first sampling time (128 ms).

— The ohmic portion of the primary voltage is bucked out by a D/A converter, therefore the remaining part can be measured in the same dynamic range as the secondary voltage.

— The dynamic range of the main 12-bit A/D converter is set automatically according to the signal level by means of binary gain setting

$$\varepsilon_s = 2^{s-1}\ \mu\text{V/bit} \tag{3}$$

and $s = 1, 2, \ldots, 6$.

— The number of measured decay curves of opposite sign is always greater than 3 (on average 8—10).

3. Data processing method

Processing of measured data takes place in two steps. The first step is a weighted averaging

$$\bar{U}_{kj} = \frac{1}{M-2} \sum_{m=2}^{M-1} \frac{U_{kj}^{m-1} - 2U_{kj}^{m} + U_{kj}^{m+1}}{4} \tag{4}$$

where $\bar{U}_{kj}$ is the weighted mean value of the voltage at t_{kj}

M is the total number of the recorded impulses

m is serial number of impulses, $2 \leqq m \leqq M-1$, impulse $m-1$ and $m+1$ have the same, impulse m the opposite polarity.

The next step is the determination of the dynamic parameters. These parameters can be determined by several methods. Probably the most simple of these is to compare the decay curves with precalculated "master curves" [HALVERSON et al. 1981]. The limits are the same as experienced in the similar interpretation of vertical electric soundings. Another method which is quite often applied is the so-called factoring. The advantage of the method is the small memory requirement easily met by programmable calculators. Its main drawback is the necessity for interactivity and subjective decisions. We ourselves used this method for several years [ERKEL, 1979]. There is, however, a further deficiency, viz. the constant which is generally present in the data cannot be determined in such a way. The processing of the decay curves of about 100 data was very time-consuming even though only a part of data was used simultaneously (samples of constant sampling rate) and there was no proof whether the approximation was the best possible or not. In possession of computers of larger memory we have turned to the computation of dynamic parameters by means of the Marquardt algorithm [MARQUARDT 1963]. Our computer program itself is the modified version of W. E. Ball's Fortran program translated to Enhanced Basic of Hewlett–Packard.

The main program has different input possibilities depending on the type of tasks. We first needed to check the parameters obtained by the interactive method. To do this we had a fairly good initial guess and expected only small changes of parameters. We then processed about 20 curves by the new program, in most cases there was in fact only a small difference between the parameter sets (less than 10%), and the number of parameters remained the same. The main task is, however, the processing of new, unprocessed data. In this case, of course, we had no initial guess and we practically did not limit the possible intervals for dynamic parameters. After performing several experiments it was found that there was no need for initial guesses, only the number of parameters was to be determined (up to 21). Initial guesses for amplitudes and time constants were calculated from the first sample, the sampling interval and

number of terms (only for curves without EM coupling), since the Marquardt algorithm provides a rapid convergence even in case of a poor initial guess. The sum of the squared differences between measured and calculated values (Φ) decreased by orders of magnitude during the first iterations, the parameters changed significantly too. After that both the sum and parameters changed only slightly as shown in *Fig. 2.* During the processing of decay curves disturbed by EM coupling or noise the demand came up to limit the interval of allowed changes. Without these limitations the parameters reached unreal values, time constants became much longer than the sampling interval, amplitudes became greater by orders of magnitude than the measured values. Such parameters are considered as unreal because of mathematical and not physical reasons; moreover the parameters did not show the same trend of change as mentioned before.

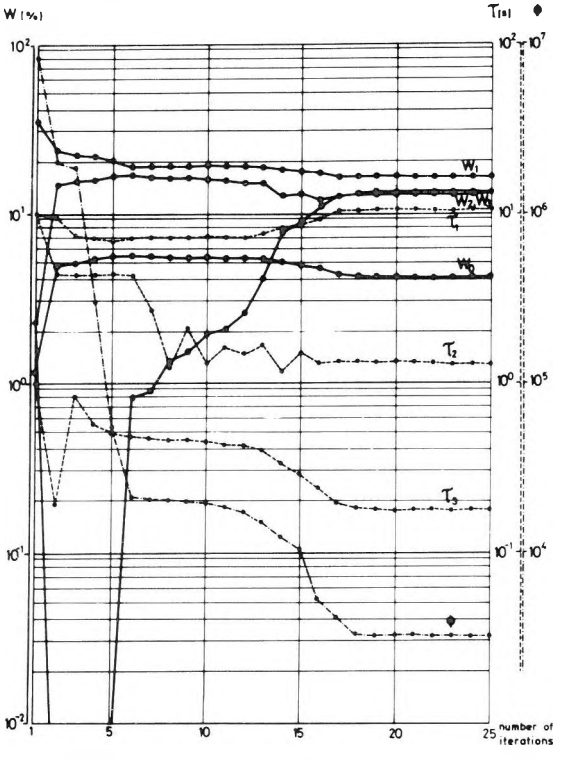

Fig. 2. Change of dynamic parameters (w_i, τ_i) and Φ during the iteration process

2. ábra. A dinamikus paraméterek (w_i, τi) és Φ változása az iterációs folyamat során

Рис. 2. Изменение динамических параметров (w_i, τ_i) и Φ в итерационном процессе

Almost every parameter changed significantly in every iteration on the one hand, Φ remained unchanged on the other hand. To approximate measured values closer than the measuring error has no practical meaning. An obvious choice would be to calculate the scattering or standard deviation of samples

belonging to the same moment, to average them in order to get a limit and stop the program if the averaged difference between measured and calculated values falls within this limit. We carried out some experiments on noisy curves and the method worked well, but not on curves with strong EM coupling. The processing of such curves requires the direct limitation of parameters; later we shall return to this problem.

We are in the middle of experiments concerning every step of data processing. For the time being stacking, digital filtering and computation of exponential parameters are carried out separately, with the possibility of software changes, but for our final aim—a microprocessor controlled system—a complete and many times checked processing system is needed.

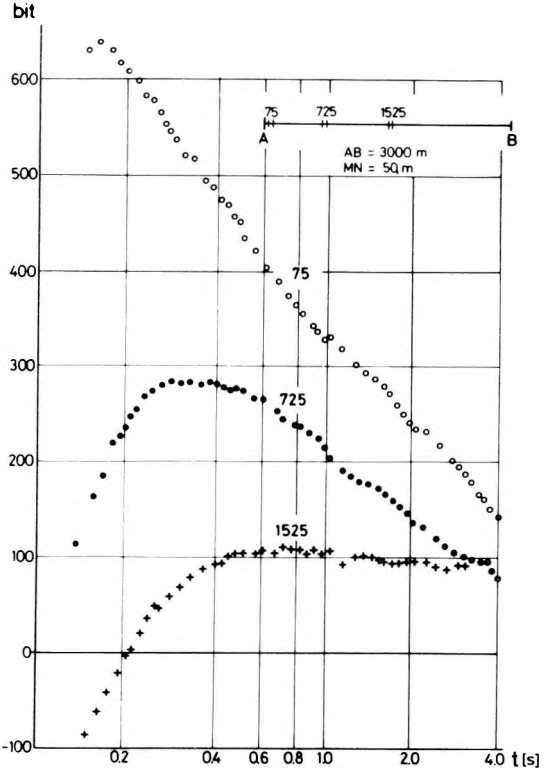

Fig. 3. Decay curves measured with long current bipole (gradient array). Apparent resistivity is about 50 Ωm along the profile

3. ábra. Hosszú áramdipóllal mért lecsengési görbék (gradiens elrendezés). A látszólagos ellenállás 50 Ωm körül van a szelvény mentén

Рис. 3. Кривые затухание, измеренные с длинним токовым диполем (градиентная установка). Кажущееся сопротивление составляет ок. 50 Ωм по профилю

4. Proper choice of the number of exponential terms

First we would like to demonstrate what kind of approximation can be made if the signal-to-noise ratio is similar to that shown in *Fig. 3*. We have found that the already mentioned difference between measured and calculated values (δ_{kj}) can best be used to characterize the approximation. It could be characterized by one number too, namely by Φ, but the distribution of δ_{kj} yields very important information. Therefore the final printout of computer processing—besides the dynamic parameters, of course—contains the plot of δ_{kj} and Φ. Two printouts are shown in *Fig. 4/a* and *b*. The very systematic, almost sine wave pattern of δ_{kj} (in logarithmic time scale) is surprising. In connection with this phenomenon the basic question concerning the decision on the number of terms necessary for the best approximation, will be discussed.

As in many other cases we have to make a compromise. Obviously the greater the number of components the better the approximation. But our aim is to use a minimum number of components. A possible solution is to start with

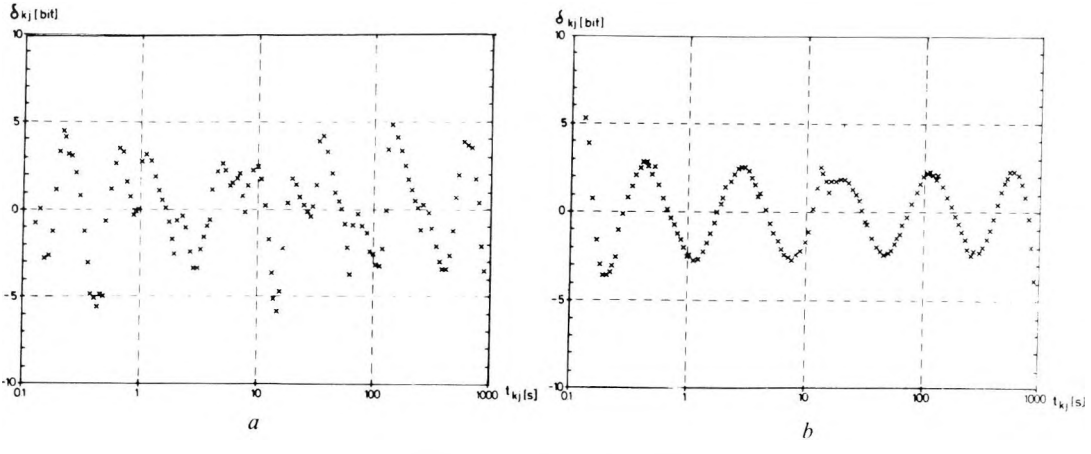

Fig. 4. Final printout of data processing
Dynamic parameters
4. ábra. Az adatfeldolgozás végeredménye
Dinamikus paraméterek

Рис. 4. Окончательный результат обработки материалов
Динамические параметры

a) $w_0 = 0.06\%$
$w_1 = 0.48\%$ $\tau_1 = -526.3$ s
$w_2 = 0.48\%$ $\tau_2 = -83.3$ s $\Phi = 810$
$w_3 = 0.37\%$ $\tau_3 = -13.51$ s
$w_4 = 0.29\%$ $\tau_4 = -2.60$ s
$w_5 = 0.34\%$ $\tau_5 = -0.035$ s

$\sum_{i=0}^{5} w_i = 2.02\%$

b) $w_0 = 0.52\%$
$w_1 = 2.18\%$ $\tau_1 = -344.8$ s
$w_2 = 1.67\%$ $\tau_2 = -50.0$ s $\Phi = 480$
$w_3 = 1.42\%$ $\tau_3 = -7.81$ s
$w_4 = 1.31\%$ $\tau_4 = -1.614$ s
$w_5 = 1.56\%$ $\tau_5 = -0.165$ s

$\sum_{i=0}^{5} w_i = 8.66\%$

only one exponential component, then to increase the number of components (N in equation 1) step by step and in the meantime to follow with attention the change of Φ and the distribution of δ_{kj}. So far as Φ can be decreased significantly by increasing N this procedure is worth being continued and finally the differences must show a randomly scattered pattern (taking into consideration the smoothing effect of the digital filtering, i.e. weighted averaging). In the course of increasing N the distribution of δ_{kj} many times displayed a pattern similar to that shown in *Fig. 4/b* It is certain it was not noise. The reason was that we did not allow enough components, but used just one less—and this bears emphasizing. The use of more components is unnecessary. This is shown in *Fig. 5.* Three components are not enough because of systematic error; four components offer the best solution; the use of $N=6$ is excessive giving an approximation which is by no means better. We have found a fairly good test for deciding the optimum number of exponential terms.

For fully automatic data processing it is easier to formulate the process in the opposite way, i.e. to start with maximum of N and to decrease it step by

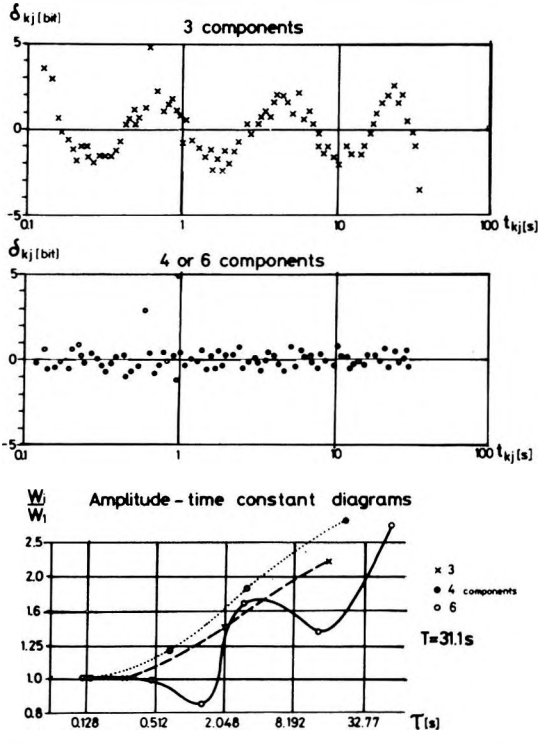

Fig. 5. Distributions of δ_{kj} and the normalized amplitude—time constant diagrams for approximations by different numbers of components

5. ábra. δ_{kj} eloszlása és a normált amplitudó—időállandó diagramok különböző számú komponenssel való közelítés esetén

Рис. 5. Распределение δ_{kj} и диаграммы нормированная амплитуда—постоянная времени при аппроксимации различным количеством составляющих

step. If Φ increases by less than 10% (or 5% or 1%) during the successive iterations one or more components could be deleted

a) the term having a time constant shorter than $t_{00}/5$,

b) terms with time constants whose ratio is less than 1.6 can be drawn together (the limit depends on the accuracy of the equipment)

c) the term having a time constant longer than 10 times the sampling interval (its amplitude is added to the constant).

The iteration process is carried on using the reduced N, Φ and the distribution of δ_{kj} should be checked again to decide whether the reduction of N was correct or not. The criteria are the same: the trend of Φ and the pattern of δ_{kj}.

5. Basis of interpretation

It is well-known that ZONGE and HUGHES [1981] have divided the Cole—Cole diagrams into three basic groups *A*, *B* and *C*, representing decreasing, horizontal and increasing types. We have arranged a similar grouping of amplitude—time constant distributions. Having a non-physical model it is obvious that amplitudes and time constants have no direct physical meaning. The distribution of amplitudes, however, is different for different sources. As the sum of w_i, i.e. the exponential amplitudes normalized to the primary signal—the apparent polarizability with 0 second delay time—sometimes yields no information, in the final plotting of results w_i values are normalized once more to the amplitude belonging to the shortest time constant as shown in *Fig. 6* (this

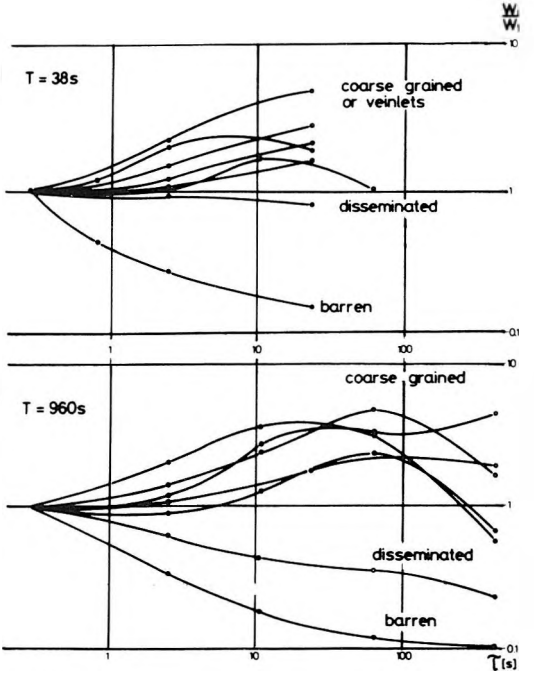

Fig. 6. Normalized amplitude—time constant diagrams obtained using short and long charging pulses (laboratory measurements)

6. ábra. Hosszú és rövid gerjesztéssel kapott normált amplitudó—időállandó diagramok (laboratóriumi mérések)

Рис. 6. Диаграммы нормированная амплитуда—постоянная времени, полученные с долгим и коротким возбуждением (лабораторные измерения)

all holds true only for EM coupling free curves or if the EM coupling term is neglected). These normalized amplitude—time constant diagrams in double logarithmic scale serve as a basis for interpretation.

Diagrams belonging to different ore types or geologic models could be found empirically only, by a number of experiments being carried out and the results being used in a statistical way.

6. Measurements on rock samples

Before going into detail about applying this method it might be useful to explain briefly the kinds of exploration tasks that we are seeking to solve by IP in Hungary. In our country the base metal occurences are linked mainly with young, hydrothermally altered Miocene—Eocene andesites and are characterized by large horizontal extent and low, uneconomical grade, at least in the depth interval of IP measurement. Within the basically pyrite mineralizations there are zones of higher grade copper-polymetallic ores, in other words we have porphyry copper deposits of poor quality. A small amount of higher grade ores can be found at the edges of the volcanic body, if the country rock was limestone or dolomite (skarn), but we have no massive ore. With regard to texture and grain size there are very fine grained disseminations, veinlets and stringers (stockwork). The highest grade ores (about 15—20%) are of veinlet type, the thickness of the fissure fillings is 3—10 mm. Therefore we have to study the decay curves of the ore types mentioned before (in our domestic work we have rarely encountered a need for sulphide—graphite discrimination).

We have carried out very many laboratory measurements on cores. In Fig. 6 amplitude—time constant diagrams of barren rock, disseminated and veinlet type mineralizations are shown (andesite matrix with pyrite, magnetite and chalcopyrite). Measurements were performed by short (58 s) and long (960 s) charging pulses. For veinlet type mineralization the amplitudes increased with increasing time constant and the trend was nearly the same for short and long charging pulses, the place of maximum depends on the length of the charging pulse. For disseminated mineralization there was no change in the amplitudes if a short charging pulse was used, the trend was slightly decreasing if long pulse was used. For barren rocks in both cases there is a rapid decrease in amplitudes. It is worth mentioning thet the shape of diagrams was influenced by the length of the charging pulse, but the basic trend remained the same for a given texture type.

In *Fig. 7* the effect of anisotropy is shown. The direction of the current flow with respect to the sample was changed during the measurements. For the sample containing only disseminated mineralization (sample B) the amplitude distribution showed no change; for samples with fissure filling (A) or oriented stringers (C) both the shape and the values of amplitudes strongly depended upon direction of current. In rock sample measurements, effects are always exaggerated, e.g. apparent polarizability values are very high, the anisotropy is

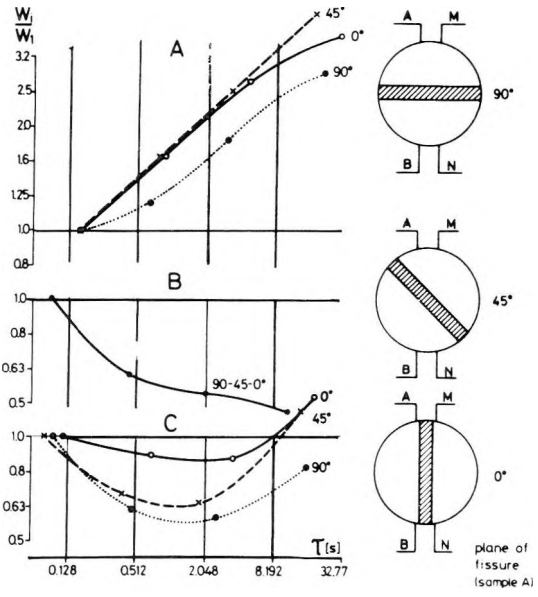

Fig. 7. Effect of anisotropy: dynamic parameters for very anisotropic (*A*), homogeneous (*B*) and moderately anisotropic (*C*) rock samples as a function of the current's direction

7. ábra. Az anizotrópia hatása: nagyon anizotróp (*A*), homogén (*B*) és mérsékelten anizotróp (*C*) kőzetminták dinamikus paraméterei az áram irányának függvényében

Рис. 7. Влияние анизотропии: динамические параметры сильно анизотропных (*A*), однородных (*B*) и умеренно анизотропных (*C*) образцов горных пород в зависимости от направления тока

very strong, the shapes of the diagrams are very different. In field measurements we could not expect the same (because of the dilution factor) so it was mandatory to carry out field measurements on geologically controlled sources too.

7. Field measurements

In a Miocene volcanic mountain AB rectangle IP measurements were made by conventional TD instruments, followed by the determination of dynamic parameters for source discrimination on anomalies only. The interpretation of decay curves measured over disseminated and veinlet type mineralizations is shown in *Fig. 8*. Because the signal-to-noise ratio was favourable we calculated the differential curves too. The apparent polarizabilities ($P_{0.5}$ measured with 32 s long charging) are nearly constant along the profile (15—17%). The derivatives of the decay curves measured with long charging pulses and the shape of the amplitude—time constant distributions are very similar. The trends of changes are the same as experienced in laboratory measurements, only the absolute values are smaller.

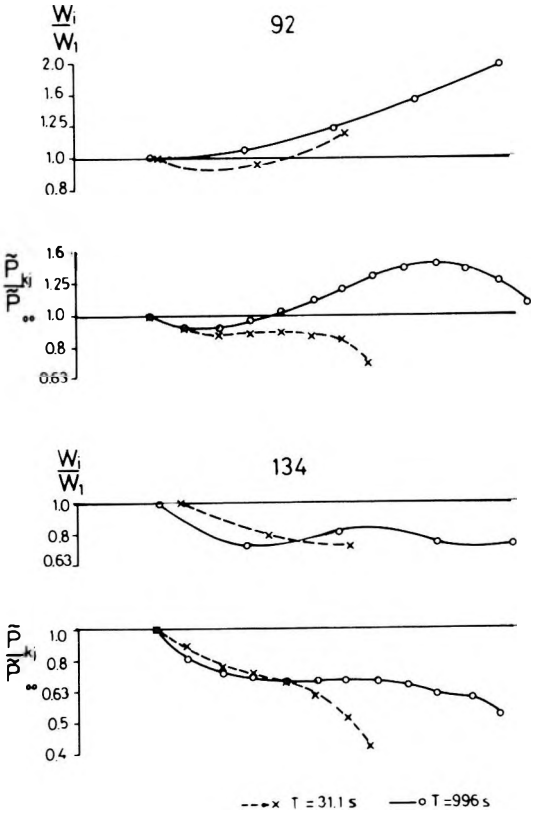

Fig. 8. Normalized amplitude—time constant (w_i/w_1) and derivative ($\tilde{P}_{kj}/\tilde{P}_{00}$) curves for veinlet (92) and disseminated (134) mineralizations obtained by different charging pulses

8. ábra. Normált amplitudó—időállandó (w_i/w_1) és derivált ($\tilde{P}_{kj}/\tilde{P}_{00}$) diagramok hálós-eres (92) és hintett (134) ércesedés esetén, különböző hosszúságú gerjesztésekkel

Рис. 8. Диаграммы нормированная амплитуда—постоянная времени (w_i/w_1) и крувые производных ($\tilde{P}_{kj}/\tilde{P}_{00}$) для жильного (92) и вкрапленного оруденения (134) при разных продолжительностях возбуждения

In the measurements shown in *Fig. 9* only the dynamic parameters could be used for source discrimination, the derivative curves were very noisy and characterless. The apparent polarizability is somewhat lower along the profile (it was the ridge of an elongated IP anomaly). It is known from drillings that the profile can be divided into two parts. On the eastern part the mineralization consists of very finely disseminated pyrite only, on the western half the grain size is somewhat coarser. The change of grain size reflects different mineral composition: the bulk of ore minerals is pyrite, the chalcopyrite content is, however, somewhat higher, but not of economic interest. The apparent polarizabilities are different at the two halves of the profile, but when IP parameters of the whole investigation area are known it is impossible to discriminate on the basis of apparent polarizability alone.

TD measurements for source discrimination were carried out by using short (31.1 s) and long (996 s) charging pulses. Of course, the measuring interval was longer when the charging pulse was longer. Decay curves of shorter pulses can be described by 3, the longer ones by 4—5 terms. If conditions were favourable (high signal-to-noise ratio) the amplitude—time constant diagrams of different charging pulses have exactly the same shape, though time constants are different (stations 98 and 116). In most cases the trend of the

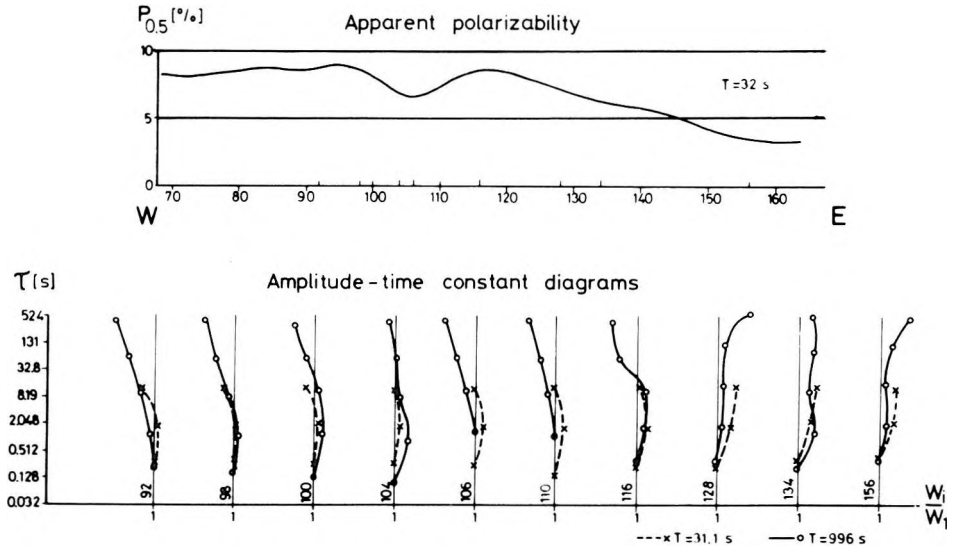

Fig. 9. Apparent polarizability and normalized amplitude—time constant diagrams along a profile with slightly different mineralizations

9. ábra. Látszólagos gerjeszthetőség és normált amplitudó—időállandó diagramok olyan szelvény mentén, ahol az ércesedés jellege kissé változik

Рис. 9. Диаграммы кажущейся поляризуемости и нормированная амплитуда—постоянная времени по профилю с небольшим изменением характера оруденения

diagrams for different charging times is similar (stations 92, 104, 156). About 10% of measurements yielded different diagrams for different charging times (stations 106, 110), mainly because of poor signal-to-noise ratio.

From field measurements two conclusions can be drawn

1) the dynamic parameters do not depend on measurement parameters, but by using long charging and measuring times more terms can be determined and the shape of the diagrams becomes unambigous,

2) the normalized amplitude—time constant diagrams obviously differ between the eastern and western parts of the profile; in the middle there is a transition zone with characterless diagrams.

Otherwise the unambiguity of dynamic parameters was also checked on these curves. By processing the same data set repeatedly, using different initial guesses and allowing a different N we finally got nearly the same values as the best approximation and the scattering of the parameters did not influence the shape of the diagrams.

8. Removal of EM coupling

We have already mentioned the problem of EM coupling. In Fig. 3 a very distorted decay curve can be seen, it is dominated over a relatively long interval

by EM coupling (curve 1525). It is more reasonable to use an exponential term to describe the EM coupling, its substantial difference being that EM coupling has a negative sign (in most cases). Our program has an option for computing negative amplitudes. We have processed decay curves measured along a profile and the results were not the best (some decay curves are shown in Fig. 3). It should be noted that the AB line of the gradient array was very long (3 km) therefore the signal-to-noise ratio was very low and only the first part of the decay curves could be used for further processing. Relatively short, noisy curves with strong EM coupling are not the best for processing and the results reflected the problems: some parameters reached unreal values. Following the changes of parameters along the profile it appeared that (see Fig. 10)

a) moving off from the current electrode the absolute value of EM coupling amplitude increases, whereas the time constant does not change,

b) amplitudes describing IP (w_0 and w_1) reached unreal values at the same distance from AB, their sum being almost the same (in other words parameters became strongly correlated),

c) at the same distance τ_1 became much longer than the sampling interval.

It was clear that because of the poor signal-to-noise ratio in the middle of the array the indirect limitation of parameters discussed before cannot be used, a direct method is needed, viz. the fixing of some parameters. We have used the averaged parameters of those parts of the profile which provided acceptable parameters for EM coupling and IP too. We allowed these parameters to fluctuate within a narrow band only. The fixed parameters were the time constants. The fixing of parameters resulted in an increase of the squared sum, but since no other possibility is available we have to accept this. The results of processing with fixed parameters reflect the changes of the depth of the polarizable rock masses covered by young sediments.

One measurement does not provide sufficient basis to draw general conclusions; there are, however, hopes of solving the EM coupling removal in TD.

Fig. 10. EM coupling removal (array is shown in Fig. 3). Prime denotes results obtained with fixed parameters and the fixed parameters themselves. For simplicity w_0 is not plotted

10. ábra. Az EM csatolás eltávolítása (az elrendezést a 3. ábra mutatja). A vessző a rögzített paraméterekkel kapott eredményeket és magukat a rögzített paramétereket jelöli. Az egyszerűség kedvéért w_0-t nem ábrázoltuk

Рис. 10. Устранение ЭМ связи (установка показана на рис. 3). Запятая показывает результаты, полученные с зафиксированными параметрами и самые зафиксированные параметры. Для простоты значение w_0 не изображено

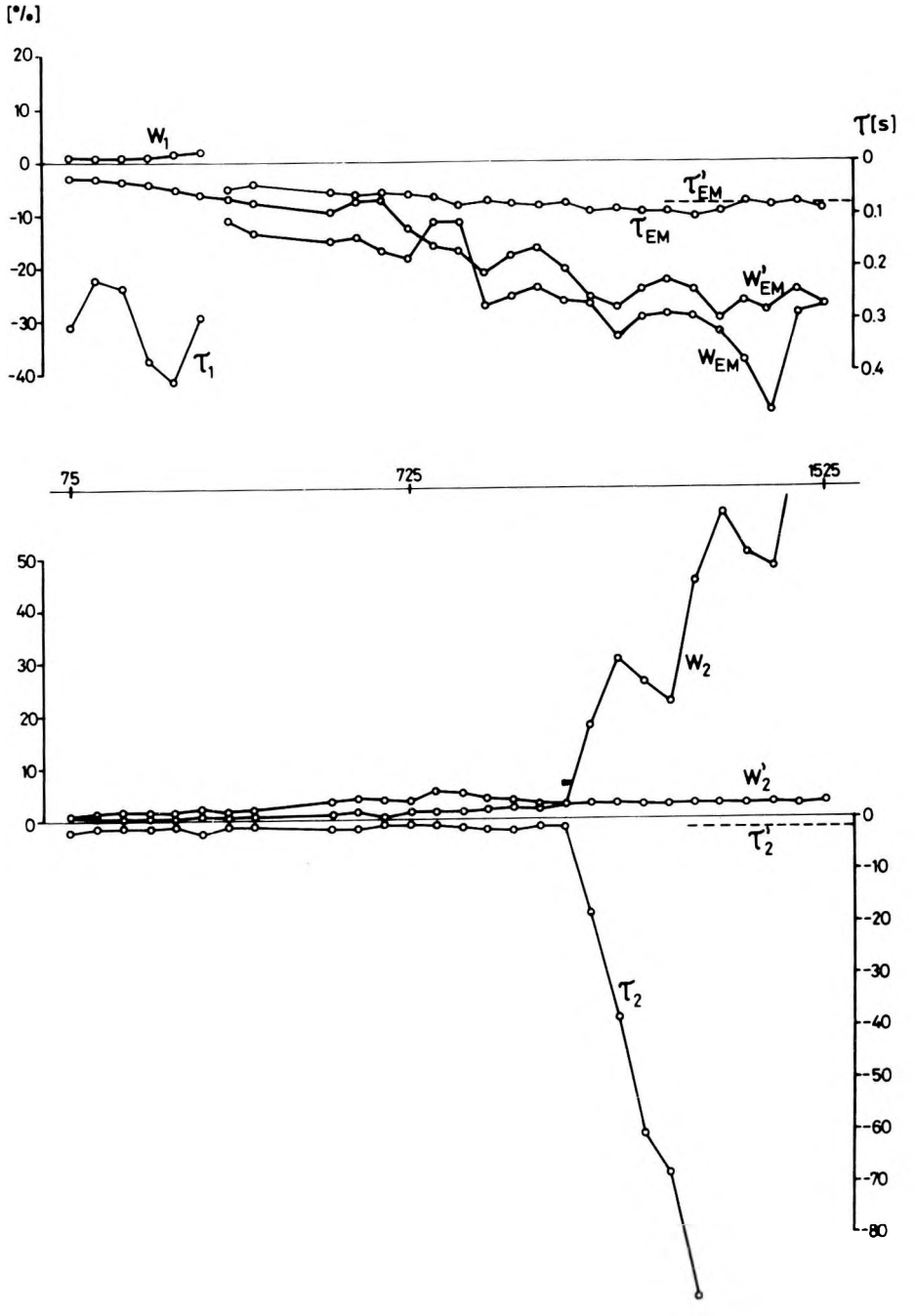
[%]
20
10
0
-10
-20
-30
-40
W1
τ1
τ'EM
τEM
W'EM
WEM
τ[s]
0
0.1
0.2
0.3
0.4
75
725
1525
50
40
30
20
10
0
W2
W'2
τ'2
τ2
-10
-20
-30
-40
-50
-60
-70
-80

9. Conclusions

The examples shown are the first successful results of a new data acquisition and processing system. The most important conclusions are as follows:

1) the data processing method is suitable to describe 80—130 samples of decay curves by a limited (7—13) number of dynamic parameters with sufficient accuracy,

2) sources of different texture really give rise to different dynamic parameter distributions and these distributions can be used for source discrimination,

3) solving of the EM coupling problem is possible,

4) further effort is needed to study the use of shorter charging times and the similarities with other methods,

5) very many laboratory and field measurements should be carried out to provide experimental data for interpretation purposes,

6) to increase production a microprocessor controlled data acquisition and processing system should be built,

7) data processing should be completed with parameter correlation and standard deviation computations.

Acknowledgement

One of the authors (L. V.) wishes to express his thanks to B. D. Smith of the United States Geological Survey for encouragement and for suggesting some useful modifications.

REFERENCES

Erkel A., Simon P. and Verő L. 1979: Measurement and interpretation of the dynamic characteristics of induced polarization decay curves. Geophysical Transactions, **25,** 61—72

Halverson M. O., Zinn W. G., McAlister E. O., Ellis R. B. and Yates W. C. 1981: Assessment of results of broad-band spectral IP field tests, in Advances in induced polarization and complex resistivity. Edited by J. S. Sumner. The University of Arizona, Tucson, Arizona, 295—344

Komarov V. A., Mikhailov G. N., Khloponina L. S., Ioffe L. M. and Smirnov A. A. 1979: Methodological guide for geoelectric system SVP 74, (in Russian) Lenuprizdat, Leningrad 32—33

Marquardt D. W. 1963: An algorithm for least-squares estimation of non-linear parameters. J. Soc. Indust. Appl. Math. **11,** 431—441

Pelton W. H., Ward S. H., Hallof P. G., Sill W. R. and Nelson P. H. 1978: Mineral discrimination and removal of inductive coupling with multifrequency IP. Geophysics, **43,** 3, 588—609

Wait J. R. 1959: The variable frequency method, in Overvoltage research and geophysical applications, edited by J. R. Wait, Pergamon Press, London, 29—49

Wong J. 1979: An electrochemical model of the induced polarization phenomenom in disseminated sulfide ores. Geophysics, **44,** 7, 1245—1265

Zonge K. L. and Hughes L. J. 1981: The complex resistivity method, in Advances in induced polarization and complex resistivity, edited by J. S. Sumner, The University of Arizona, Tucson, Arizona, 163—208

IDŐTARTOMÁNYBAN DOLGOZÓ BERENDEZÉS ÉS MÓDSZER A GERJESZTETT POLARIZÁCIÓS HATÓK MINŐSÍTÉSÉRE

CSÖRGEI JÓZSEF, ERKEL ANDRÁS, VERŐ LÁSZLÓ

A gerjesztett polarizációs módszerben új eredményeket főleg a frekvencia tartományban érnek el és a publikációkban csak röviden utalnak az idő tartományra. Egy szélessávú digitális magnetofonnal végzett időtartománybeli, laboratóriumi és terepi mérések adatfeldolgozási és értelmezési problémáit tárgyaljuk. A berendezés rövid műszaki leírását a Marquardt algoritmuson alapuló adatfeldolgozás ismertetése követi. A nagyon széles időtartományban mért lecsengési görbéket exponenciális tagok összegével közelítjük. Az amplitudók és időállandók laboratóriumi és terepi mérésekből kapott eloszlását mutatjuk be. Kőzetmintákon és földtanilag jól ismert anomáliákon végzett mérések szolgálnak az értelmezés alapjául. A módszer az elektromágneses csatolás kiküszöbölését is lehetővé teszi.

АППАРАТУРА И МЕТОДИКА ДЛЯ РАЗЛИЧЕНИЯ ИСТОЧНИКОВ ВЫЗВАННОЙ ПОЛЯРИЗАЦИИ В ВРЕМЕННОМ ДИАПАЗОНЕ

Й. ЧЁРГЕИ, А. ЭРКЕЛ, Л. ВЕРЁ

По методу ВП новые результаты достигаются прежде всего в частотном диапазоне, а относительно временного диапазона в публикациях даются только короткие ссылки. В работе обсуждаются проблемы обработки и интерпретации данных лабораторных и полевых измерений, проведенных при помощи широкополосного цифрового магнитофона в временном диапазоне. Краткому описанию аппаратуры следует изложение процедуры обработки данных, основанной на алгоритме Маркарда. Кривые затухания, замеренные в очень широком диапазоне времени, аппроксимируются суммой экспоненциальных членов. Приводится распределение амплитуд и постоянных времени, полученных по лабораторным и полевым измерениям. В основу интерпретации лежат измерения, произведенные на образцах горных пород и геологически хорошо изученных аномалиях. Метод также позволяет устранить электромагнитную связь.